

## Investigation of ultimate energy capabilities of powerful ultraviolet (370 nm) matrix emitters: current and temperature factors

© A.E. Chernyakov<sup>1</sup>, A.L. Zakgeim<sup>1</sup>, A.E. Ivanov<sup>1</sup>, N.A. Talnishnikh<sup>1</sup>, E.I. Shabunina<sup>2</sup>

<sup>1</sup> Submicron Heterostructures for Microelectronics, Research & Engineering Center, RAS, St. Petersburg, Russia

<sup>2</sup> Ioffe Institute, St. Petersburg, Russia  
e-mail: chernyakov@mail.ioffe.ru

Received April 05, 2025

Revised August 28, 2025

Accepted October 24, 2025

An experimental study was conducted on the energy, spectral, and thermal characteristics of a powerful ultraviolet ( $\lambda = 370$  nm) matrix light-emitting diode CBM-120-UV based on AlInGaN. In the current range of 1–18 A mapping of brightness, temperature, emission spectrum, and current distributions was performed across both the matrix area and individual emitting elements. Temperature gradients across the matrix area were observed at currents above 9 A, yet these did not lead to noticeable current distribution nonuniformity among the parallel-connected elements, despite the known temperature dependence of forward voltage. The obtained results are crucial for assessing the ultimate energy capabilities of UV emitters, optimizing their design, and determining operational modes.

**Keywords:** AlInGaN, light diode, UV, matrix emitter, temperature gradients, electrical luminescence, short-range field of radiation.

DOI: 10.61011/EOS.2025.11.62919.8042-25

Ultraviolet (UV) emitters in the UV-A range (315–400 nm) find wide application across various fields of science and technology — from photolithography and polymerization to medical diagnostics, fluorescent analysis, and biological research [1–3]. Compared to traditional UV lamp sources, light-emitting diodes (LEDs) based on AlInGaN heterostructures offer several advantages: compactness, mechanical robustness, absence of toxic substances, and precise spectral tuning capability. However, as the power of such emitters increases, thermal and current limitations become increasingly significant, potentially reducing device efficiency, stability, and lifetime [4–6].

Matrix LED assemblies of high density, where individual LEDs are connected in parallel and operate under high-current conditions, are of particular interest. In such systems, complex thermal interactions and current redistribution occur among individual emitting chips, driven by local temperature effects and variations in electrical characteristics. A critical factor is the temperature dependence of the forward voltage on each chip, which leads to positive feedback between heating and current. Additionally, intra-chip effects such as current crowding in the contact region exacerbate thermal loads and may cause local overheating and device degradation [7–9].

Despite existing theoretical models and individual experimental data, a detailed investigation of the interrelationships among current distribution, temperature profile, and optical characteristics in powerful UV-emitting matrices remains a relevant task. This work aims to provide a comprehensive analysis of thermal and electroluminescent processes using the industrial CBM-120-UV emitter ( $\lambda = 370$  nm) as an

example, with the goal of identifying ultimate operating regimes and limitations imposed by design and heat dissipation conditions.

### Experiment

The subject of investigation was the commercially available powerful UV matrix light-emitting diode CBM-120-UV (Luminus Devices, USA) with an emission wavelength of  $\lambda \sim 370$  nm; its appearance is shown in Fig. 1. The emitter comprises 12 densely packed AlInGaN/GaN-based chips connected in parallel and mounted on a common copper substrate (size  $28 \times 28$  mm, thickness 3.5 mm) serving as a heat sink. The chips are arranged in an  $4 \times 3$  configuration with a gap of  $100 \mu\text{m}$ , between them; the active area of each chip is approximately  $1 \text{ mm}^2$ . The housing design includes a thermistor for temperature measurement and mounting holes for attachment to an external heatsink [10,11].

Experimental studies were conducted over a current range from 1 to 18 A. Optical characteristics (spectrum and integrated emission power) were measured using the OL770 LED Test and Measurement System spectroradiometer (Optronic Laboratories, USA). Spatial distributions of spectral and power parameters across the matrix surface were determined using an Avantes 2048 spectrometer (Avantes BV, Netherlands) equipped with a fiber-optic input featuring micropositioners, enabling individual chip analysis through scanning [12].

Temperature distributions (mapping) were assessed using the infrared (IR) thermal vision microscope UTK-1 (IPP SB



**Figure 1.** Appearance of the CBM-120-UV matrix light-emitting diode emitter. Adapted from [10].

RAS). The resulting maps enabled analysis of temperature gradients both between chips and within individual chips, as well as determination of temperature dependencies on current and heat sink design features [13].

Special attention was given to correlations among temperature, current, and optical power distributions, which are crucial for the development and operation of powerful semiconductor UV sources [14].

For enhanced measurement accuracy with the UTK-1, preliminary calibration of the emissivity of various matrix structural elements and individual chips was performed by heating in a precision thermostat with a step of  $5^{\circ}\text{C}$  and recording the corresponding IR signal intensity (results shown in Fig. 2, *b*), accounting for material-specific emissivity variations. The technique is detailed in [15].

## Results and discussion

At currents above 9 A (corresponding to approximately 0.75 A and density  $\sim 75\text{ A/cm}^2$  per chip), a pronounced temperature gradient begins to form within the emitting matrix. Thermal vision mapping revealed that at 15 A (per specification), the temperature of central chips averages 5 K higher than that of peripheral chips. This arises from less efficient lateral heat dissipation in the substrate's central region. Fig. 2, *a* shows the near-field self-IR emission of the matrix; due to symmetry, only a quarter of the sample is depicted, including three peripheral and one central chip. For clarity, emission intensity is color-coded from blue (2100 bit) to red (3000 bit).

Considering the temperature sensitivity of forward voltage  $U_f = f(T)$  (temperature coefficient at low currents

$\text{TCU} \approx -0.9\text{ mV/K}$ ), the elevated temperature of central chips reduces their forward voltage. In parallel-connected chips, this causes current redistribution favoring the central chips. In the established stationary regime, this redistribution is counterbalanced by opposing effects, resulting in stable temperature and current gradients: central chips operate under elevated current and thermal loads. An increase in current through central chips was expected to boost their optical power. However, despite higher temperatures, suppression of the quantum efficiency of radiative recombination offsets this effect, with no noticeable increase in optical power observed.

Accordingly, spectral characteristics of emission from central and peripheral chips were primarily investigated for comparison.

Despite the temperature gradient, spectral analysis showed that at both 9 A and 15 A, the peak wavelength and spectral width remain identical for central and peripheral regions (Fig. 3). Moreover, emission spectral shapes proved identical, confirming spectral distribution stability amid the observed temperature field nonuniformities. Emitted power was assessed in relative units via the spectral curve integral, enabling comparison of individual chip contributions to total optical power at different current levels.

Analysis of near-field emission further revealed nonuniformities due to current crowding effects in the contact metallization region and beneath it. This effect depends on chip design and contact topology, leading to local current density increases that may exacerbate droop in quantum efficiency with current („efficiency droop“) and contribute to localized structure degradation [16,17]. In our case, noticeable current crowding was observed at operating current densities through individual chips up to  $\sim 150\text{ A/cm}^2$ .

## Conclusion

The experimental investigation of electroluminescent, electrical, and thermal characteristics of the powerful UV matrix emitter CBM-120-UV ( $\lambda \approx 370\text{ nm}$ ) over a wide range of operating currents established the influence of operating regimes on optical and thermal characteristics of both the entire matrix and its constituent chips, depending on geometric positioning, and identified factors limiting its ultimate energy capabilities. It was shown that at currents above 9 A (0.75 A per chip), temperature gradients within  $5^{\circ}\text{C}$  form in the matrix (maximum absolute heating at 15 A —  $110^{\circ}\text{C}$ ), potentially leading to nonuniform current distribution between central and peripheral chips due to the temperature dependence of forward voltage. The resulting positive feedback between temperature and current stabilizes a somewhat nonuniform current distribution favoring central chips as operating current increases. In theory, this could alter spectral and power characteristics of individual chips in near-field emission and, consequently, yield complex integral current-electroluminescence dependencies.

However, detailed near-field emission analysis demonstrated that up to limiting currents of approximately 15 A,

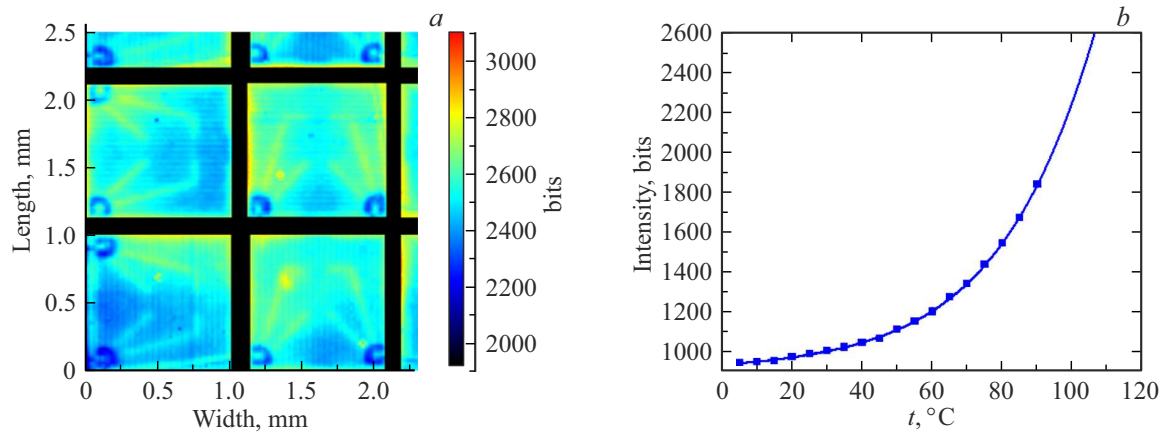


**Figure 2.** IR emission distribution map across the UV matrix (a), calibration curve — dependence of central chip IR emission on temperature (b).

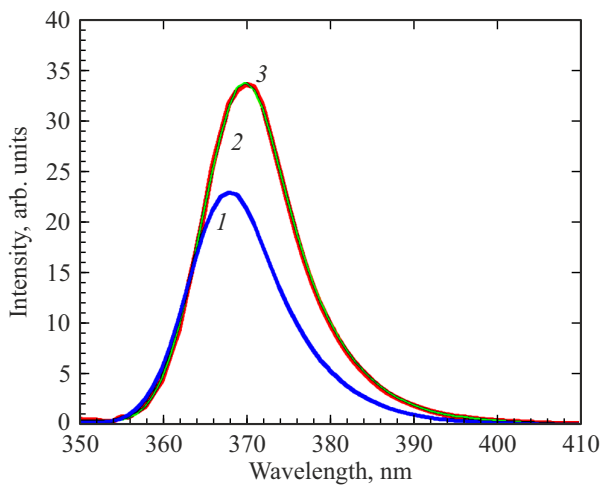


**Figure 3.** Emission spectra from individual chips: 1 — from central and peripheral,  $I = 9$  A; 2 — central,  $I = 15$  A; 3 — peripheral,  $I = 15$  A.

the peak wavelength and spectral width of emission remain identical for central and peripheral chips, as does their emission power. This seemingly paradoxical result, given the thermally mapped gradients, can be explained by several factors: 1) relatively modest temperature gradient magnitudes, 2) partial compensation of current redistribution to central chips by their efficiency reduction due to heating, 3) current-induced spectral stability characteristics of low-In-content AlInGa<sub>N</sub> UV heterostructures.

The conducted studies demonstrate the feasibility of combined high-spatial-resolution analysis of temperature and emission fields in powerful matrix UV LED sources, enabling assessment of nominal and ultimate operating modes. The latter are of particular interest, as many applications are constrained by the need for high specific irradiance fluxes. In this metric, UV emitters currently lag behind visible and IR counterparts.

The studies were performed at the common use center „Hardware Components of Radio Photonics and Nanoelectronics: Technology, Diagnostics, Metrology“.

#### Conflict of interest

The authors declare that they have no conflict of interest.

#### References

- [1] M. Shur, A. Zukauskas. Proc. IEEE, **93** (10), 1691 (2005).
- [2] S. Pimputkar, J.S. Speck, S.P. DenBaars, S. Nakamura. Nature Photonics, **3**, 180 (2009).
- [3] A. Khan, K. Balakrishnan, T. Katona. Nature Photonics, **2**, 77 (2008).
- [4] A.E. Chernyakov et al. Microelectronics Reliability, **79**, 457 (2017).
- [5] M. Bogdanov et al. Phys. Status Solidi C, **5** (6), 2070 (2008).
- [6] M. Meneghini et al. Phys. Status Solidi A, **207** (5), 1084 (2010).
- [7] E.F. Schubert. *Light-Emitting Diodes*, 2nd ed. (Cambridge University Press, 2006).
- [8] J.J. Wierer, J.Y. Tsao, D.S. Sizov. Laser & Photonics Reviews, **7** (6), 963 (2013).
- [9] N. Narendran et al. Journal of Crystal Growth, **268** (3–4), 449 (2004).
- [10] CBM-120-UV Product Datasheet. Luminus Devices Inc.
- [11] S. Pimputkar et al. Nature Photonics, **3**, 180 (2009).
- [12] A.E. Chernyakov et al. Microelectronics Reliability, **79**, 457 (2017).
- [13] M. Bogdanov et al. Phys. Status Solidi C, **5** (6), 2070 (2008).
- [14] A. Khan, K. Balakrishnan, T. Katona. Nature Photonics, **2**, 77 (2008).
- [15] A.E. Chernyakov, E.S. Polovinkin, A.A. Novikov, S.V. Kapustin, A.S. Kuznecov. FTP4 (3), 685-690 (2010). (in Russian).
- [16] A.E. Chernyakov et al. Microelectronics Reliability, **79**, 457 (2017).
- [17] M. Bogdanov et al. Phys. Status Solidi C, **5** (6), 2070 (2008).

Translated by J.Savelyeva